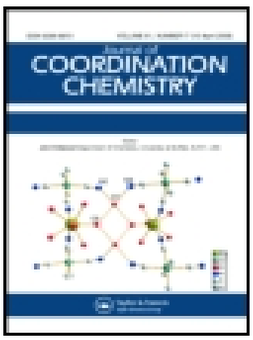

Journal of Coordination Chemistry

ISSN: 0095-8972 (Print) 1029-0389 (Online) Journal homepage: http://www.tandfonline.com/loi/gcoo20

Preparation, characterization, and structural analysis of d^8 palladium and platinum compounds containing amino acid ester derivatized diimine ligands. Observation of liquid crystal behavior

Richard S. Herrick, Christopher J. Ziegler, Tang Ding, Janet Shaw, Iwona Wrona, Matthew Beaver, Joshua Giguere, Caroline Maus & Peter Müller

To cite this article: Richard S. Herrick, Christopher J. Ziegler, Tang Ding, Janet Shaw, Iwona Wrona, Matthew Beaver, Joshua Giguere, Caroline Maus & Peter Müller (2017): Preparation, characterization, and structural analysis of d^8 palladium and platinum compounds containing amino acid ester derivatized diimine ligands. Observation of liquid crystal behavior, Journal of Coordination Chemistry, DOI: 10.1080/00958972.2017.1383602

To link to this article: http://dx.doi.org/10.1080/00958972.2017.1383602

Published online: 09 Oct 2017.

JOURNAL OF COORDINATION CHEMISTRY, 2017
https://doi.org/10.1080/00958972.2017.1383602

Taylor & Francis
Taylor & Francis Group

Preparation, characterization, and structural analysis of d^8 palladium and platinum compounds containing amino acid ester derivatized diimine ligands. Observation of liquid crystal behavior

Richard S. Herrick[a], Christopher J. Ziegler[b], Tang Ding[b], Janet Shaw[c], Iwona Wrona[a], Matthew Beaver[a], Joshua Giguere[a], Caroline Maus[a] and Peter Müller[d]

[a]Department of Chemistry, College of the Holy Cross, Worcester, MA, USA; [b]Department of Chemistry, University of Akron, Akron, OH, USA; [c]Department of Chemistry and Biochemistry, Kennesaw State University, Kennesaw, GA, USA; [d]Department of Chemistry, Massachusetts Institute of Technology, Cambridge, MA, USA

ABSTRACT

Eight new compounds, $M(pyca(CH_2)_xCOOR)Cl_2$, M = Pd, Pt; R = Me, Et; x = 2, 3, 5, 11, were prepared. The resulting new complexes were characterized by ^1H and ^{13}C NMR spectroscopy and each was also structurally elucidated by X-ray crystallography. The compounds share general structural features, but there are differences in the alignment of the alkyl chain; as the chain lengthens, the chain straightens relative to the plane of the metal complex. For the dodecanoic ester derivatives, a nearly linear alkyl chain was observed. These longer alkyl derivatives show mesogenic behavior.

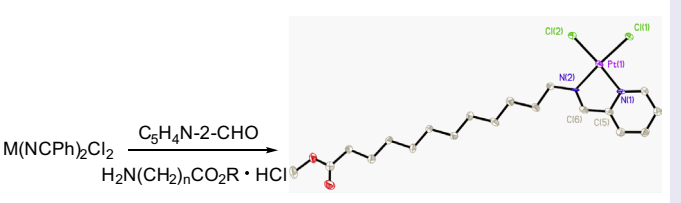

ARTICLE HISTORY
Received 19 July 2017
Accepted 22 August 2017

KEYWORDS
Amino acid; crystal structure; diimine; palladium; platinum

1. Introduction

The study of α-diimine compounds, formed by condensation of pyridine-2-carboxaldehyde with amino acids or amino acid esters, has provided surprising results for d^6 carbonyl systems. These compounds, which are typically highly stable, can be used as chromophores for dye applications as well as for the generation of bioorganometallic conjugate systems. Accordingly, this interest has driven investigations into the fundamental synthetic chemistry of these systems. For example, we and others have produced and characterized a series of $M(CO)_4$(pyca-Xxx-OR) (M = Mo,W) [1–4] complexes, where pyca is the pyridine-2-

CONTACT Richard S. Herrick rherrick@holycross.edu

carbaldehyde imine fragment ($C_5H_4NCH = N$), using esters of amino acids and pyridine aldehyde. When $W(CO)_4(piperidine)_2$ was treated with α-amino acids and pyridine-2-carboxaldehyde, condensation was accompanied by decarboxylation for H-L-Ala-OH or H-L-Asp-OH (Scheme 1) [5]. Longer chain amino acids did not decarboxylate, and dipeptides were created with the metal fragment acting as protecting group.

Similarly, treatment of $Mo(CO)_4(pip)_2$ and glyoxal with amino acid esters in the presence of NEt_3 produces diastereomeric mixtures following racemization at the amino acid α-carbon [6]. In the racemization process, base-assisted proton removal at the α-carbon occurs followed by re-protonation of the trigonal planar α-carbon. The observed racemization and decarboxylation processes mimic the reactivity of vitamin B6 decarboxylase enzymes with the metal fragment playing the same role as a proton [7].

Additionally, we and others have observed similar metal-mediated Schiff base formation in $Re(CO)_3$ based compounds [8–17]. The generation of imino pyridine complexes of $Re(CO)_3$ was originally achieved via stepwise synthesis of the Schiff base followed by chelation of the ligand to the metal. Miguel and coworkers isolated the first pyridine-2-carboxaldehyde complex of $Re(CO)_3$, $Re(CO)_3$(pyca)Br, and demonstrated that this compound reacts readily with a variety of primary amines, including anilines, amino acids, and peptides [1, 8]. In our past work, we investigated the reaction of $Re(CO)_5Cl$ with pyridine-2-carboxyaldehdye and amino esters [12] and demonstrated that $Re(CO)_3(H_2O)_3^+$ reacts under one-pot conditions with pyridine-2-carboxaldehyde and the amino acids glycine and alanine, affording C_2-symmetric dimers [17]. We also combined this ligand scaffold with hydrazine to link metal centers [15, 16] and used it to label short peptides [14].

Given these interesting results obtained for d^6 systems, we decided to extend this work to square planar d^8 systems. Numerous palladium and platinum d^8 pyca complexes have been reported in the literature [18–21]. Typically the uses that were examined for these compounds involved catalytic applications, though there was one report of a platinum complex with a pyca ligand containing a glucose molecule that was tested for antitumor activity [21].

Herein, we report the synthesis and spectroscopic characterization for condensation reactions of palladium and platinum salts in the presence of pyridine-2-carboxaldehyde and aminocarboxylic esters separated by alkyl chains of varying lengths. We present the

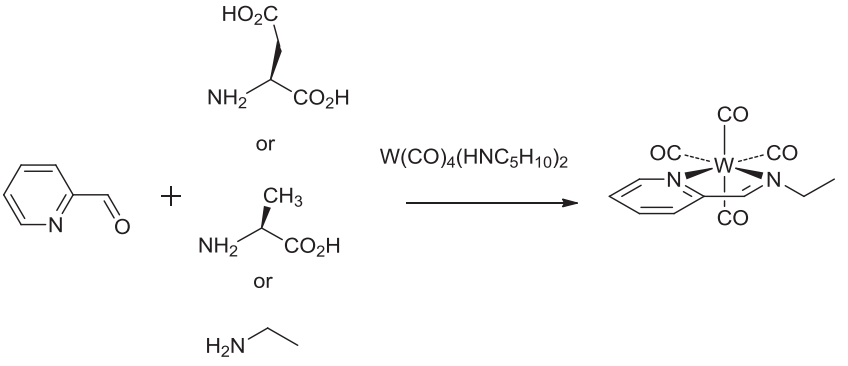

Scheme 1. Preparation of $W(CO)_4$(pyca-Et) via three different amines.

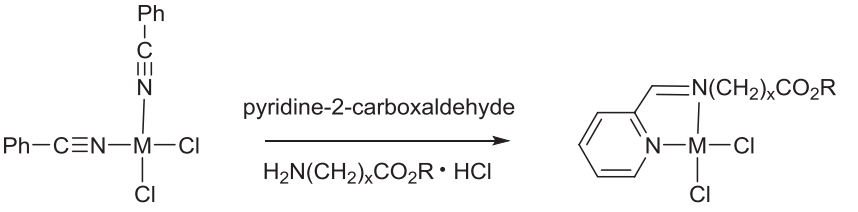

No.	Pd	Pt	x	R
1	**a**	**b**	2	Et
2	**a**	**b**	3	Me
3	**a**	**b**	5	Me
4	**a**	**b**	11	Me

Scheme 2. Reaction scheme and numbering used for compounds reported.

preparation of $M(pyca(CH_2)_xCO_2Me)Cl_2$, M = Pd, Pt; R = Me, Et; x = 2, 3, 5, 11 (Scheme 2) and report on the crystal structures of the eight compounds. Comparison of the structures demonstrates that in the shorter derivatives the alkyl chain is nearly orthogonal to the plane of the metal complex whereas the alkyl chains of the longer derivatives become linear, leading away from the planes of the metal complexes. Both the platinum and palladium complexes exhibit similar characteristics, and in the case of the longest carbon chain molecules, the resultant compounds exhibit mesogenic properties.

2. Experimental

2.1. Spectroscopic measurements

NMR spectra were recorded on a Varian 400 MHz spectrometer. IR spectra were recorded on a Nicolet Series II Magna-IR 750 spectrometer. Elemental analyses were performed by Atlantic Microlab of Norcross, GA (USA). Thermal analyses were performed on a TGA V5.1A Dupont 2100 instrument from room temperature to 600 °C with a heating rate of 10 °C min^{-1} under an atmosphere of dinitrogen. Differential scanning calorimetry (DSC) was conducted at 10 °C min^{-1} using a Perkin-Elmer PYRIS Diamond DSC device with an Intracooler 2P apparatus. Data were processed with the DataMax for Windows software program.

2.2. Materials and methods

$M(C_6H_5CN)_2Cl_2$, M = Pd, Pt, H-β-Ala-OEt and methanol were obtained from Strem Chemicals and used without purification. Amino acid ester hydrochloride salts were obtained from Bachem. GABA-OMe·HCl, 1,6-Aminohexanoic acid methyl ester and 1,12-aminododecanoic acid methyl ester were each prepared as the HCl salt from the amino acids using a method described previously [4].

2.3. X-ray crystal structure determinations 1–8

Diffraction data for **3b** were collected at 100 K on a Siemens Platform three-circle diffractometer coupled to a Bruker-AXS Smart Apex CCD detector with graphite-monochromated Mo Kα radiation (λ = 0.71073 Å), performing φ- and ω-scans. For the remaining structures, diffraction data were collected at 100 K on a Bruker SMART APEX CCD-based X-ray diffractometer system equipped with a Mo-target X-ray tube (λ = 0.71073 Å). Data reduction was performed with SAINT [22]; absorption corrections were made using SADABS [23]. The structures were solved by direct methods using SHELXS [24], and all non-hydrogen atoms were located from the initial solutions. All structures were refined against F^2 on all data by full-matrix least squares with SHELXL [24] following established refinement strategies [25]. All hydrogen positions were visible in the difference Fourier synthesis; hydrogens were included in calculated positions and subsequently refined using a riding model.

For all eight structures, the relevant parameters for crystal data, data collection, structure solution and refinement are summarized in Table 1, and selected bond lengths and angles are summarized in Tables 2 and 3.

2.4. Synthesis

All new palladium and platinum compounds were prepared in a similar fashion. Below is a representative synthesis for the preparation of GABA-methyl ester imino-2-pyridine platinum(II) chloride, Pt(pyca-GABA-OMe)Cl_2, **2b**. Pyridine-2-carboxaldehyde (0.0283 g, 2.64×10^{-4} mol), and GABA-OMe·HCl (0.0406 g, 2.64×10^{-4} moles) were added to 15 mL of degassed methanol and stirred for twenty minutes. $Pt(C_6H_5CN)_2Cl_2$ (0.125 g, 2.64×10^{-4} mol) was added to the solution and the solution was refluxed under nitrogen overnight. The solvent was evaporated and the solid was recrystallized multiple times from a small amount of cooled methanol or via a solvent diffusion process using CH_2Cl_2 and hexanes. Pt(pyca-GABA-OMe)Cl_2, **2b**, was isolated as a bright orange solid in 54% yield. Crystals suitable for X-ray diffraction were grown by evaporation from methanolic solutions. ^{1}H and ^{13}C NMR resonances for **1–4** are shown in Tables 4 and 5, respectively.

1a: 52% yield. m.p. 209–211 °C. Anal. Calc. for $C_{11}H_{14}Cl_2N_2O_2Pd$: C, 34.44; H, 3.68; N, 7.30. Found: C, 34.19; H, 3.61; N, 7.14%.

1b: 54% yield. m.p. 205–206 °C. Anal. Calc. for $C_{11}H_{14}Cl_2N_2O_2Pt$: C, 27.98; H, 2.99; N, 5.93. Found: C, 27.94; H, 2.90; N, 5.82%.

2a: 54% yield. m.p. 197–199 °C. Anal. Calc. for $C_{11}H_{14}Cl_2N_2O_2Pd$: C, 34.44; H, 3.68; N, 7.30. Found: C, 34.37; H, 3.64; N, 7.23%.

2b: 50%. m.p. 154–155 °C. Anal. Calc. for $C_{11}H_{14}Cl_2N_2O_2Pt$: C, 28.03; H, 2.99; N, 5.95. Found: C, 28.11 H, 3.06; N, 5.91%.

3a: 53% yield. m.p. 145 °C (d). Anal. Calc. for $C_{13}H_{18}Cl_2N_2O_2Pd{\cdot}CH_2Cl_2$: C, 33.87; H, 4.06; N, 5.64. Found: C, 34.41; H, 4.25; N, 5.85.

3b: 23% yield. m.p. 148 °C (d). Anal. Calc. for $C_{13}H_{18}Cl_2N_2O_2Pt{\cdot}CH_2Cl_2$: C, 28.82; H, 3.45; N, 4.81. Found: C, 29.04; H, 3.40; N, 4.99.

4a: 34% yield. m.p. 150–152 °C. Anal. Calc. for $C_{11}H_{14}Cl_2N_2O_2Pd$: C, 46.03; H, 6.10; N, 5.65. Found: C, 45.77; H, 6.10; N, 5.50%.

4b: 34% yield. m.p. 119–120 °C. Anal. Calc. for $C_{11}H_{14}Cl_2N_2O_2Pt$: C, 39.05; H, 5.17; N, 4.79. Found: C, 39.33; H, 5.15; N, 4.89%.

Table 1. X-ray data collection and structure parameters for **1–4**.

Compound	**1a**	**1b**	**2a**	**2b**
Empirical formula	$PdCl_2C_{11}H_{14}N_2O_2$	$PtCl_2C_{11}H_{14}N_2O_2$	$PdCl_2C_{11}H_{14}N_2O_2$	$PtCl_2C_{11}H_{14}N_2O_2$
Formula weight	383.54	472.23	383.54	472.23
Crystal system	Monoclinic	Monoclinic	Monoclinic	Monoclinic
Space group	P2(1)/c	P2(1)/c	P2(1)/c	P2(1)/c
Unit cell dimensions	$a = 10.7827(11)$ Å $\alpha = 90°$ $b = 16.6415(17)$ Å $\beta = 99.461(2)°$ $c = 7.8238(8)$ Å $\gamma = 90°$	$a = 10.8298(13)$ Å $\alpha = 90°$ $b = 16.662(2)$ Å $\beta = 100.316(2)°$ $c = 7.8046(10)$ Å $\gamma = 90°$	$a = 11.2288(13)$ Å $\alpha = 90°$ $b = 16.4142(19)$ Å $\beta = 93.758(2)°$ $c = 7.3876(8)$ Å $\gamma = 90°$	$a = 11.154(2)$ Å $\alpha = 90°$ $b = 16.416(3)$ Å $\beta = 93.352(3)°$ $c = 7.3883(13)$ Å $\gamma = 90°$
Volume	1384.8(2) $Å^3$	1385.6(2) $Å^3$	1358.7(3) $Å^3$	1350.6(4) $Å^3$
Z	4	4	4	4
Density (calculated)	1.858 Mg/m^3	2.264 Mg/m^3	1.875 Mg/m^3	2.322 Mg/m^3
Absorption coefficient	1.737 mm^{-1}	10.507 mm^{-1}	1.753 mm^{-1}	10.779 mm^{-1}
$F(000)$	760	888	760	888
Crystal size	$0.60 \times 0.40 \times 0.01$ mm^3	$0.30 \times 0.06 \times 0.01$ mm^3	$0.25 \times 0.10 \times 0.05$ mm^3	$0.40 \times 0.20 \times 0.05$ mm^3
Theta range for data collection	1.92–28.30°	2.27–28.26°	1.82–28.27°	1.83–28.30°
Index ranges	$-14 \le h \le 14$, $-21 \le k \le 21$, $-10 \le l \le 10$	$-14 \le h \le 14$, $-21 \le k \le 21$, $-10 \le l \le 10$	$-14 \le h \le 14$, $-21 \le k \le 21$, $-9 \le l \le 9$	$-14 \le h \le 14$, $-20 \le k \le 21$, $-9 \le l \le 9$
Reflections collected	12,098	11,601	11,510	10,909
Independent reflections	3317 [R(int) = 0.0470]	3321 [R(int) = 0.0642]	3198 [R(int) = 0.0497]	3143 [R(int) = 0.0705]
Completeness to theta	97.0%	96.4%	95.2%	93.9%
Data/restraints/parameters	3317/0/219	3321/0/164	3198/0/164	3143/0/164
Goodness-of-fit on F^2	1.050	1.054	1.112	1.014
Final R indices [I>2sigma(I)]	R1 = 0.0326, wR2 = 0.0765	R1 = 0.0487, wR2 = 0.1157	R1 = 0.0333, wR2 = 0.0756	R1 = 0.0417, wR2 = 0.1033
R indices (all data)	R1 = 0.0427, wR2 = 0.0801	R1 = 0.0549, wR2 = 0.1189	R1 = 0.0373, wR2 = 0.0774	R1 = 0.0501, wR2 = 0.1074
Largest diff. peak and hole	1.153 and −0.655 $e.A^{-3}$	3.890 and −4.756 $e.A^{-3}$	0.928 and −0.734 $e.A^{-3}$	3.438 and −2.573 $e.A^{-3}$

(*Continued*)

Table 1. (*Continued*).

Compound	**3a**	**3b**	**4a**	**4b**
Empirical formula	$PdCl_2C_{13}H_{18}N_2O_2$	$PdCl_2C_{13}H_{18}N_2O_2$	$PdCl_2C_{19}H_{30}N_2O_2$	$P5Cl_2C_{19}H_{30}N_2O_2$
Formula weight	411.59	500.28	495.75	584.44
Crystal system	Monoclinic	Monoclinic	Monoclinic	Monoclinic
Space group	C2/2	P2(1)/c	P2(1)/n	P2(1)/n
Unit cell dimensions	$a = 14.269(6)$ Å $\alpha = 90°$ $b = 13.866(6)$ Å $\beta = 96.448(7)°$ $c = 15.544(7)$ Å $\gamma = 90°$	$a = 9.4958(6)$ Å $\alpha = 90°$ $b = 7.0438(4)$ Å $\beta = 98.1180(10)°$ $c = 23.2761(15)$ Å $\gamma = 90°$	$a = 9.3882(16)$ Å $\alpha = 90°$ $b = 7.7803(13)$ Å $\beta = 95.536(3)°$ $c = 29.460(5)$ Å $\gamma = 90°$	$a = 9.4045(10)$ Å $\alpha = 90°$ $b = 7.7668(8)$ Å $\beta = 95.337(2)°$ $c = 29.425(3)$ Å $\gamma = 90°$
Volume	3056(2) Å^3	1541.26(16) Å^3	2141.8(6) Å^3	2140.0(4) Å^3
Z	8	4	4	4
Density (calculated)	1.789 Mg/m^3	2.156 Mg/m^3	1.537 Mg/m^3	1.814 Mg/m^3
Absorption coefficient	1.566 mm^{-1}	9.452 mm^{-1}	1.131 mm^{-1}	6.822 mm^{-1}
F(000)	1648	952	1016	1144
Crystal size	$0.50 \times 0.01 \times 0.01$ mm^3	$0.25 \times 0.10 \times 0.06$ mm^3	$0.50 \times 0.35 \times 0.05$ mm^3	$0.17 \times 0.08 \times 0.02$ mm^3
Theta range for data collection	2.05–27.00°	2.60–29.13°	2.22–24.99°	1.39–28.29°
Index ranges	$-18 \le h \le 18$, $-17 \le k \le 17$, $-19 \le l \le 19$	$-13 \le h \le 13$, $-9 \le k \le 9$, $-31 \le l \le 31$	$-11 \le h \le 11$, $-9 \le k \le 9$, $-34 \le l \le 35$	$-12 \le h \le 12$, $-10 \le k \le 10$, $-38 \le l \le 38$
Reflections collected	11,766	32,296	14,657	17,955
Independent reflections	3148 [*R*(int) = 0.1427]	4139 [*R*(int) = 0.0354]	3769 [*R*(int) = 0.0435]	5150 [*R*(int) = 0.0603]
Completeness to theta	99.9%	100.0%	99.9%	96.7%
Data/restraints/parameters	3148/0/182	4139/0/182	3769/0/236	5150/0/236
Goodness-of-fit on F^2	0.983	1.064	1.379	1.238
Final *R* indices [I>2sigma(I)]	R1 = 0.0632, wR2 = 0.1443	R1 = 0.0159, wR2 = 0.0386	R1 = 0.0603, wR2 = 0.1147	R1 = 0.0584, wR2 = 0.1392
R indices (all data)	R1 = 0.0973, wR2 = 0.1588	R1 = 0.0178, wR2 = 0.0398	R1 = 0.0642, wR2 = 0.1160	R1 = 0.0614, wR2 = 0.1408
Largest diff. peak and hole	1.122 and −1.467 e.A^{-3}	0.977 and −0.610 e.A^{-3}	1.112 and −1.248 e.A^{-3}	3.100 and −2.997 e.A^{-3}

Table 2. Selected bond distances and angles for **1a**–**4a**.

	1a	2a	3a	4a
Pd–Cl	2.2825(8), 2.2897(8)	2.2819(8), 2.2988(7)	2.276(2), 2.2762(17)	2.2718(15), 2.2959(14)
Pd–N_{pyr}	2.019(2)	2.021(2)	2.018(6)	2.029(5)
Pd–N_{imine}	2.020(2)	2.021(2)	2.005(5)	2.027(5)
Cl–Pd–Cl	91.16(3)	90.37(3)	90.37(7)	90.59(5)
Cl–Pd–N_{pyr}	94.10(7)	94.56(7)	94.00(17)	94.50(14)
Cl–Pd–N_{imine}	94.25(7)	94.24(7)	94.32(19)	93.70(14)
N–Pd–N	80.51(10)	80.81(10)	81.4(2)	81.23(18)

Table 3. Selected bond distances and angles for **1b**–**4b**.

	1b	2b	3b	4b
Pt–Cl	2.2997(19), .3001(19)	2.2850(19), 2.2977(18)	2.2926(5), 2.3052(6)	2.277(2), 2.3026(19)
Pt–N_{pyr}	2.012(6)	2.003(6)	2.0139(18)	2.030(7)
Pt–N_{imine}	2.010(6)	2.009(6)	2.009(2)	2.010(6)
Cl–Pt–Cl	90.23(7)	89.38(7)	89.22(2)	89.53(7)
Cl–Pt–N_{pyr}	94.30(18)	94.85(17)	95.02(5)	95.13(19)
Cl–Pt–N_{imine}	95.25(18)	95.27(18)	95.40(6)	94.84(19)
N–Pt–N	80.2(2)	80.5(2)	80.36(7)	80.5(3)

3. Results and discussion

3.1. Synthesis of compounds

Pyridine-2-carboxaldehyde and the appropriate α,ω-amino ester hydrochloride salt were stirred in methanol under nitrogen at room temperature in a one pot reaction for 20 min. No special precautions with respect to excluding atmospheric oxygen or water were required. Addition of $M(C_6H_5CN)_2Cl_2$, M=Pd, Pt, and reflux overnight produced the products as yellow to orange solids. Purification was best accomplished by multiple recrystallizations from slowly cooled methanol with purified, air-stable compounds obtained in moderate yields. The products are the α,ω-amino ester conjugate complexes **1**–**4**.

3.2. X-ray structure elucidation

The structure of each new compound was elucidated by single crystal X-ray methods (Figures 1 and 2). Each compound shows a roughly square planar arrangement of the pyridine nitrogen, imine nitrogen, and two chlorides placed in a *cis*-configuration around the central metal. Selected bond distances are shown in Table 2 for the palladium compounds and Table 3 for the platinum compounds. The measured distances and angles for all compounds are similar, with all M-Cl distances being between 2.28–2.30 Å, the M-N distances between 2.00 and 2.03 Å, the Cl-M-Cl and N-M-N angles spanning ~89–91° and ~80–81°, respectively.

The β-alanine derivatives and GABA structures (**1a**,**b** and **2a**,**b**) show very similar molecular arrangements; the alkyl chain of each of these structures aligns so that it is essentially perpendicular to the diimine ligand plane. Several other structures of compounds with the pyca-β-ala-OR ligand have been reported with a similar characteristic alignment of the alkyl chain, including $Mo(CO)_4$(pyca-β-Ala-OEt) [4], $Re(CO)_3Cl$(pyca-β-Ala-OEt) [12], $W(CO)_4$(pyca-β-Ala-Val-OMe) [5] and [Hpip][$Mo(CO)_4$(pyca-β-Ala-O^-)] [2].

Table 4. ^{1}H NMR[a] for **1–4**.

	NC_5H_4	*H*–C=N	α-CH_2	Other CH_2's	OR
1a	9.08 d (5.7), 7.99 m, 8.47 m, 8.27 d (6.6))	8.77 s	4.04 t (6.6)	3.05 t (6.6)	4.18 q (7.0), 1.28 t (7.0)
1b	9.48 d (5.2), 8.03 m, 8.50 m, 8.31 d (6.8)	9.33 s	4.33 t (6.7)	3.98 t (6.7)	4.16 q (7.0), 1.27 t (7.0)
2a	8.91 d (5.2), 7.82 m, 8.32 m, 8.04 m	8.55 s	3.69 t (6.8)	2.00 m, 2.33 m	3.54 s
2b	9.32 d (5.4), 7.86 t (7.3), 8.34 t (7.8), 8.05 d (7.4)	9.13 s	3.98 t (6.8)	2.04 m, 2.41 m	3.54 s
3a	8.91 d (5.6), 7.81 t (6.6), 8.30 t (7.8), 8.05 d (7.4)	8.60 s	3.66 t (7.0)	2.28 m, 1.72 m, 1.51 m, 1.26 m	3.53 s
3b	8.91 d (5.6), 7.82 t (7.4), 8.30 t (7.8), 8.05 d (7.4)	8.60 s	3.98 t (7.0)	2.28 m, 1.72 m, 1.52 m, 1.25 m	3.53 s
4a[b]	8.92 d (5.5), 7.81 t (7.4), 8.29 t (7.8), 8.03 d (8.2)	8.55 s	3.98 t (8.0)	2.23 m, 1.71 m, 1.46 m, 1.24–1.20 m (14H)	3.53 s
4b[b]	9.36 d (5.2), 8.37 m, 8.10 t (6.8), 7.90 (m)	9.17 s	3.98 t (8.4)	2.27 m, 1.81 m, 1.50 m, 1.30 m, 1.23–1.20 m (12H)	3.54 s

[a]Recorded in $CDCl_3$ unless otherwise indicated.
[b]Spectrum recorded in d_6-DMSO.

Table 5. ^{13}C NMR[a] for **1–4**.

	C on py	H–*C*=N	*C*=O	α-*C*	Other *C*H_2's	O*R*
1a	156.6, 156.5, 142.4, 129.8, 129.4	171.4	173.6	61.3	34.8	61.8, 14.2
1b	157.7, 150.1, 141.8, 130.3, 129.6	171.4	173.2	61.3	35.1	61.9, 14.2
2a	156.6, 150.7, 142.0, 129.2, 129.0	172.6	173.4	58.8	30.9, 25.9	52.1
2b	156.4, 148.9, 142.3, 129.0, 128.5	171.5	172.8	58.2	30.1, 25.6	51.4
3a	156.5, 150.7, 142.0, 129.2, 128.9	172.1	173.9	59.5	33.7, 30.2, 25.9, 24.6	51.9
3b	157.6, 149.6, 141.3, 129.7, 129.0	171.6	173.4	59.6	33.6, 30.6, 25.7, 24.6	51.9
4a[b]	156.3, 150.7, 142.0, 129.2. 128.9	172.0	174.1	59.7	33.9, 30.6, 29.6, 29.5, 29.3, 29.2, 29.1, 27.6, 26.4, 25.1	59.7
4b[b]	157.6, 149.6, 141.4, 129.7, 129.0	171.4	174	59.9	33.9, 30.9, 29.6, 29.5, 29.4, 29.3, 29.2, 29.1, 26.4, 25.1	59.9

[a]Recorded in $CDCl_3$ unless otherwise indicated.
[b]Spectrum recorded in d_6-DMSO.

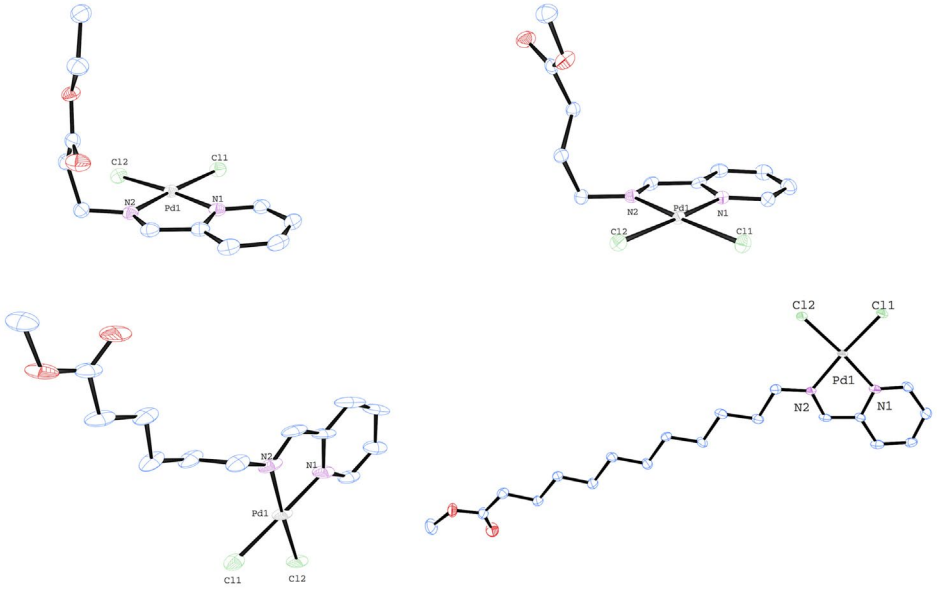

Figure 1. The structures of **1a** (top left), **2a** (top right), **3a** (bottom left), and **4a** (bottom right) with 50% thermal ellipsoids. Hydrogens have been omitted for clarity.

The increasing length of the alkyl chains affects the relative conformations of the structures. Compounds **1a**,**b** and **2a**,**b** each show an alkyl chain that is bent at a near 90° angle from the M(pyca) plane. Compounds **3a**,**b** show the hexanoic acid chain arranged in more linear arrangements that still contain some kink in the chain structure. The other Pd and Pt pairs of compounds are very similar in structure, but **3a**,**b** are slightly different from each other.

Compounds **4a**,**b** are isostructural and display a remarkable co-planarity with linear alkyl chains aligned with the plane formed by the metal complex. The angle between the plane formed by the pyca ligand, metal and chlorides and the plane of the alkyl chain is ~11.1° for **4a** and ~7.8° for **4b**. The ester group deviates from the alkyl chain plane by ~21.0° for **4a** and ~26.9° for **4b**. A similar elongated alkyl chain was observed in the structure of undecanoic acid derivative, $Re(CO)_3(pyca(CH_2)_{10}CO_2H)Br$ [26]. Two related palladium compounds,

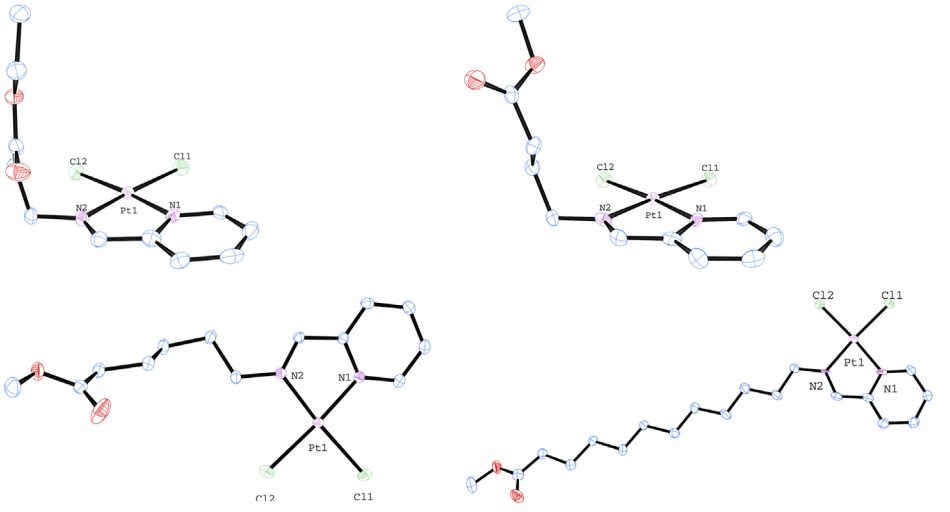

Figure 2. The structures of **1b** (top left), **2b** (top right), **3b** (bottom left), and **4b** (bottom right) with 50% thermal ellipsoids. Hydrogens have been omitted for clarity.

$Pd(pyca(CH_2)_nCH_3)Cl_2$ (n = 7, 11) show similar planar structures and extended alkyl chains [27, 28].

In the solid state, **1a**,**b** pack with stacking of the planes formed by the pyridine imines. The alkyl chains alternate in their orientations, pointing above and below these planes. As a result, the solid state is comprised of separate domains of alkyl groups and of diimine bound metal centers. Compounds **2a**,**b** arrange in a nearly identical fashion, forming stacks of square planar metal centers, alternating directions in the alkyl groups, and with alternating domains of alkyl chains and metal complexes. In **3a**,**b** changes to the solid state also appear. Compound **3b** shares many of the same features as **1a**,**b** and **2a**,**b** and exhibits clearly separated alkyl domains and metal complex domains. In contrast, **3a**, which has alkyl chains that are nearly co-linear with the plane of the metal complex, does not form separate domain structures in the solid state. Instead, the alkyl groups stack on top of the square planar metal complex regions, forming an interwoven structure in the solid state. The primary difference between **3a** and **3b** is in the orientation of the alkyl group; **3a** has an akyl region that is primarily perpendicular to the plane of the metal complex, whereas **3b** has a co-linear alkyl chain.

In **4a**,**b** major differences are observed when compared to the shorter chain complexes. First, as seen in **3b**, the alkyl chains interlace with the square planes, and there is no domain separation between these two regions of the molecules. Also, the pattern in which the molecules pack in the solid state differs from that seen in the smaller chain analogs. Compounds **4a**,**b** both show a herringbone-type pattern (Figure 3) which is markedly altered from the linear stacking patterns observed in **1a**,**b**, **2a**,**b**, and **3a**,**b**.

The two previously reported palladium compounds that display an extended alkyl chain [27, 28] pack differently from each other and also differently than **4a**,**b**. Each packs in sheets with each square plane lined up and alkyl chains pointing in the same direction. The octyl derivative forms sheets with the square planes offset from the square planes of the next layer below it. The sheets are arrayed in an ABCA pattern as each layer lies exactly over the

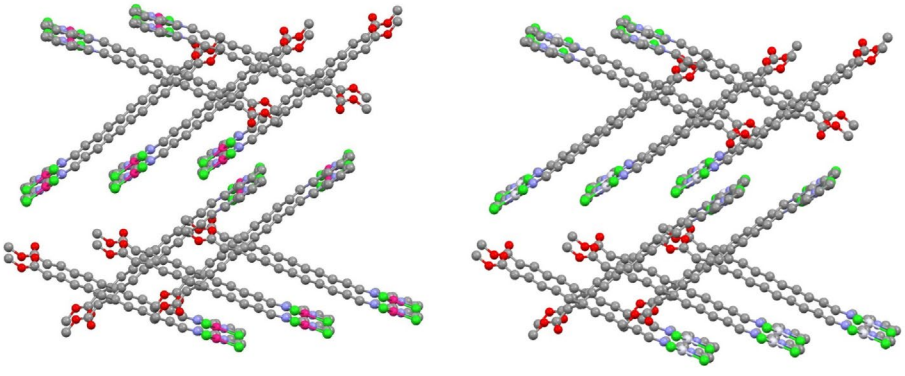

Figure 3. Packing diagrams with hydrogens omitted for clarity for **4a** (left) and **4b** (right).

layer three below it. The dodecyl derivative also has planar sheets; two sheets have alkyl chains pointing in one direction and in the next two sheets they point in the other direction. In each pair of sheets, the square planes in one sheet are offset from the square planes in the adjacent sheet.

3.3. Spectroscopic characterization

^{1}H and ^{13}C NMR spectra were acquired for all of the compounds reported. All spectra agree in detail with their proposed structures. In each compound, the imine proton appears as a singlet in each spectrum between 8.5 and 9.4 ppm while the imine carbon appears at 171–173 ppm. The amide carbonyl carbon appears between 172 and 174 ppm. Pyridine resonances were appropriate, and the methylene resonances were observed as expected in both the ^{1}H and ^{13}C NMR spectra. The amino ester functionalities occur in expected regions for all compounds, indicating that the ligand remains intact.

3.4. DSC and TGA measurements

Compounds **4a** and **4b** each form waxy crystals with melting points significantly lower than their lower molecular weight congeners. We suspected that these complexes would exhibit liquid crystalline behavior due to the presence of the long aliphatic chains. The study of metallomesogens has grown into a large field of investigation, and many palladium and platinum complexes with liquid crystalline properties have been presented in the literature [29–34]. As a preliminary evaluation of the mesogenic properties of **4a** and **4b**, we examined these compounds by thermogravimetric analysis (TGA) and by differential scanning calorimetry (DSC). TGA scans revealed that both compounds are thermally stable to ~180 °C for **4a** and ~200 °C for **4b**. Our DSC analysis showed that both compounds also undergo transitions at temperatures lower than their melting points; **4a** and **4b** melt at 159 °C and 149 °C, respectively. In addition, a liquid crystalline phase is observed for both compounds. For **4a**, a transition is observed at 113 °C, which upon cooling takes place at 77 °C. In **4b**, this transition to a liquid crystal takes place at a slightly higher temperature (~123 °C) while the cooling transition is the same as in **4a**.

4. Conclusion

This study was undertaken with the goal of preparing and characterizing new amino ester conjugates of Pd(II) and Pt(II). Eight new compounds with linear amino ester alkyl chains of varying length were prepared. Each was fully characterized and structurally elucidated. It was found that as the chain length increased, the compounds became more linear and change their mode of packing. For the dodecanoic ester compounds, a herringbone packing arrangement is observed, in contrast to that seen for analogous octane and dodecane iminopyridine palladium complexes. Additionally, for the dodecaonoic ester derivatives, mesogenic behavior was observed. Further work is planned to explore the structural behavior that was observed in these compounds.

Supplementary material

CCDC 896733–896740 contains the supplementary crystallographic data for this paper. These data can be obtained free of charge from the Cambridge Crystallographic Data Center via www.ccdc.cam.ac.uk/data_request/cif.

Disclosure statement

No potential conflict of interest was reported by the authors.

Funding

Richard S. Herrick and Christopher J. Ziegler acknowledge the National Institutes of Health [grant number R15 GM083322] for funds used in this work.

References

[1] C.M. Alvarez, R. Garcia-Rodriguez, D. Miguel. *Dalton Trans.*, 3546 (2007).
[2] R. Garcia-Rodriguez, D. Miguel. *Dalton Trans.*, 1218 (2006).
[3] C.M. Alvarez, L.A. Garcia-Escudero, R. Garcia-Rodriguez, D. Miguel. *Dalton Trans.*, 2556 (2013).
[4] R.S. Herrick, K.L. Houde, J.S. McDowell, L.P. Kiczek, G. Bonavia. *J. Organomet. Chem.*, **589**, 29 (1999).
[5] R.S. Herrick, J. Dupont, I. Wrona, J. Pilloni, M. Beaver, M. Benotti, F. Powers, C.J. Ziegler. *J. Organomet. Chem.*, **692**, 1226 (2007).
[6] R.S. Herrick, C.J. Ziegler, H. Bohan, M. Corey, M. Eskander, J. Giguere, N. McMicken, I.E. Wrona. *J. Organomet. Chem.*, **687**, 178 (2003).
[7] A.E. Martell. *Accts. Chem. Res.*, **22**, 115 (1989).
[8] C.M. Álvarez, R. García-Rodríguez, D. Miguel. *Inorg. Chem.*, **51**, 2984 (2012).
[9] C.M. Alvarez, R. Garcia-Rodriguez, D. Miguel. *Dalton Trans.*, 963 (2016).
[10] M. Grzegorczyk, A. Kapturkiewicz, F.W. Sanjuan-Szklarz. *Inorg. Chem. Commun.*, **46**, 103 (2014).
[11] R. Stichauer, A. Helmers, J. Bremer, M. Rohdenburg, A. Wark, E. Lork, M. Vogt. *Organometallics*, **36**, 839 (2017).
[12] R.S. Herrick, I. Wrona, N. McMicken, G. Jones, C.J. Ziegler, J. Shaw. *J. Organomet. Chem.*, **689**, 4848 (2004).
[13] A. Hasheminasab, J.T. Engle, J. Bass, R.S. Herrick, C.J. Ziegler. *Eur. J. Inorg. Chem.*, **2014**, 2643 (2014).
[14] K. Chanawanno, J. Caporoso, V. Kondeti, S. Paruchuri, T.C. Leeper, R.S. Herrick, C.J. Ziegler. *Dalton Trans.*, 11452 (2014).
[15] A. Hasheminasab, H.M. Rhoda, L.A. Crandall, J.T. Ayers, V.N. Nemykin, R.S. Herrick, C.J. Ziegler. *Dalton Trans.*, 17268 (2015).

[16] K. Chanawanno, H.M. Rhoda, A. Hasheminasab, L.A. Crandall, A.J. King, R.S. Herrick, V.N. Nemykin, C.J. Ziegler. *J. Organomet. Chem.*, **818**, 145 (2016).
[17] H. Qayyum, R.S. Herrick, C.J. Ziegler. *Dalton Trans.*, 7442 (2011).
[18] S. Dehghanpour, A. Mahmoudi, S. Rostami. *Polyhedron*, **29**, 2190 (2010).
[19] J. Kuwabara, D. Takeuchi, K. Osakada. *Polyhedron*, **28**, 2459 (2009).
[20] A. Saha Roy, P. Saha, P. Mitra, S. Sundar Maity, S. Ghosh, P. Ghosh. *Dalton Trans.*, 7375 (2011).
[21] M.E. Cucciolito, L.R. Del, F.P. Fanizzi, D. Migoni, G. Roviello, F. Ruffo. *Inorg. Chim. Acta*, **363**, 741 (2010).
[22] J.L. Chambers, *SAINT 7.23*, Bruker-AXS, Inc., Madison, Wisconsin, USA (2005).
[23] G.M. Sheldrick. *SADABS*, Bruker AXS Inc., Madison, WI (2009).
[24] G.M. Sheldrick, *SHELXTL, Crystallographic Software Package, Version 6.10*, Bruker-AXS, Madison, WI (2000).
[25] P. Müller. *Crystallogr. Rev.*, **15**, 57 (2009).
[26] C.M. Jung, W. Kraus, P. Leibnitz, H.-J. Pietzsch, J. Kropp, H. Spies. *Eur. J. Inorg. Chem.*, **2002**, 1219 (2002).
[27] R. Chen, J. Bacsa, S.F. Mapolie. *Inorg. Chem. Commun.*, **5**, 724 (2002).
[28] R. Chen, J. Bacsa, S.F. Mapolie. *Polyhedron*, **22**, 2855 (2003).
[29] M.J. Baena, P. Espinet, C.L. Folcia, J. Ortega. *Inorg. Chem.*, **49**, 8904 (2010).
[30] C. Chien, C.-J. Chen, H.-S. Sheu, G.-H. Lee, C.K. Lai. *Tetrahedron*, **66**, 3583 (2010).
[31] B.-M. Jung, Y.-D. Huang, J.-Y. Chang. *Liq. Cryst.*, **37**, 85 (2010).
[32] K. Venkatesan, P.H.J. Kouwer, S. Yagi, P. Müller, T.M. Swager. *J. Mater. Chem.*, **18**, 400 (2008).
[33] Y. Wang, Q. Chen, Y. Li, Y. Liu, H. Tan, J. Yu, M. Zhu, H. Wu, W. Zhu, Y. Cao. *J. Phys. Chem. C*, **116**, 5908 (2012).
[34] Y. Wang, Y. Liu, J. Luo, H. Qi, X. Li, M. Nin, M. Liu, D. Shi, W. Zhu, Y. Cao. *Dalton Trans.*, 5046 (2011).